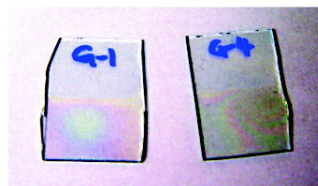
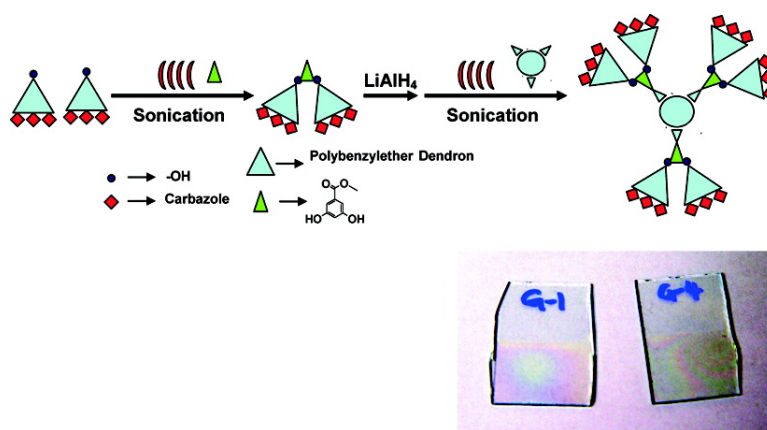


Investigating Carbazole Jacketed Precursor Dendrimers: Sonochemical Synthesis, Characterization, and Electrochemical Crosslinking Properties

Prasad Taranekar, Timothy Fulghum, Derek Patton,
Ramakrishna Ponnampati, Gabriel Clyde, and Rigoberto Advincula

J. Am. Chem. Soc., **2007**, 129 (41), 12537-12548 • DOI: 10.1021/ja074007t

Downloaded from <http://pubs.acs.org> on December 16, 2008



More About This Article

Additional resources and features associated with this article are available within the HTML version:

- Supporting Information
- Links to the 6 articles that cite this article, as of the time of this article download
- Access to high resolution figures
- Links to articles and content related to this article
- Copyright permission to reproduce figures and/or text from this article

[View the Full Text HTML](#)

Investigating Carbazole Jacketed Precursor Dendrimers: Sonochemical Synthesis, Characterization, and Electrochemical Crosslinking Properties

Prasad Taranekar, Timothy Fulghum, Derek Patton, Ramakrishna Ponnampati, Gabriel Clyde, and Rigoberto Advincula*

Contribution from the Department of Chemistry and Department of Chemical Engineering, University of Houston, Houston, Texas 77024

Received June 2, 2007; E-mail: radvincula@uh.edu

Abstract: Precursor carbazole terminated dendrons and dendrimers up to generation four (G4-D) were synthesized using a convergent approach. Sonication as a means of facilitating organic reactions in dendrimer chemistry was explored resulting in very facile and very fast (up to 50×) reaction times compared to those using traditional reflux conditions. The limits of peripheral group functionality were explored as a function of generation. The electrochemical cross-linking of the dendrimers as thin films revealed unusual cyclic voltammetry (CV) behavior depending upon the generations, which were significantly different from their linear counterpart, Poly(*N*-vinylcarbazole) (PVK). G1-D showed a higher extent of *intermolecular* cross-linking while G4-D showed a higher extent of *intramolecular* cross-linking. The formed films were optically clear and possess superior energy band gap properties making them an alternative candidate over PVK for future hole-transport layer materials in electro-optical devices.

Introduction

Electroactive polymer based dendrimers are of current interest for developing new generation organic material devices and other photonic applications.¹ Compared to well-known conjugated linear chain polymers, the unusual electronic and photophysical properties of conjugated dendrimers, for example, exciton and charge localization phenomena,^{2a,b} generation-dependent carrier mobility,^{2c} and cross-linking phenomenon,^{2d,e} are also of broad fundamental interest. Individual dendrimers and dendrimeric functional groups at polymer chain ends or in well-defined segments can determine the ultimate properties of macromolecules, providing highly controlled materials systems.³ For this purpose, several approaches have been attempted and reported, including incorporation of functional units into the periphery, the branching units, and the interior core of a dendrimer using various synthetic methodologies.⁴

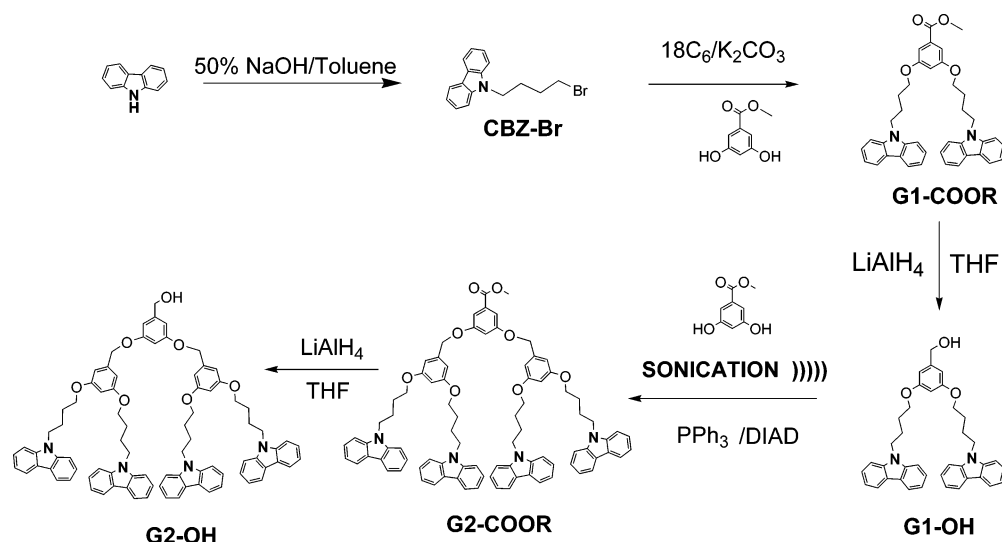
Polymers based on carbazole units are interesting because of their role in electrochromic devices, hole transport layers, microcavity photoconduction, electroxerography, and as photovoltaic components which can provide a very efficient matrix

for current carrier transport.⁵ Most organic semiconductors are understood as one-dimensional conductors because the electrons (or holes) mainly travel through conjugated chains or stacks of π -conjugated molecules.⁶ As such, a combination of complementary conjugated functional units into the periphery, branching units, and interior core of a dendrimer should give unique structure–property relationships. The three-dimensional scaffold of dendrimers would allow additional control over the structure and morphology of these materials. This could lead to interesting new properties and, conversely, identify new insight into dendrimer structure–property relationships such as electronic processes, inter- and intramolecular cross-linking, band gap tunability, and interfacial effects.⁷ With reference to the precursor polymer concept for synthesizing conjugated polymers⁸ and the desire to observe new optoelectronic effects from functional dendrimers, we have synthesized various generations of poly-(benzyl ether) type dendrimers functionalized with carbazole at the periphery and benzene-1,3,5-tricarboxylic as a core material. In the process, we have discovered and utilized a

- (1) (a) Furuta, P.; Brooks, J.; Thompson, M. E.; Fréchet, J. M. J. *J. Am. Chem. Soc.* **2003**, *125*, 13165. (b) Kwon, T. W.; Alam, M. M.; Jenekhe, S. A. *Chem. Mater.* **2004**, *16* (23), 4657. (c) Grayson, S. M.; Fréchet, J. M. J. *Chem. Rev.* **2001**, *101*, 3819.
- (2) (a) Wang, Y.; Ranasinghe, M. I.; Goodson, T. *J. Am. Chem. Soc.* **2003**, *125*, 9562. (b) Kopelman, R.; Shortreed, M.; Shi, Z. Y.; Tan, W.; Xu, Z.; Moore, J. S.; Bar-Haim, A.; Klafter, J. *Phys. Rev. Lett.* **1997**, *78*, 1239. (c) Lupton, J. M.; Samuel, I. D. W.; Beavington, R.; Burn, P. L.; Bassler, H. *Adv. Mater.* **2001**, *13*, 258. (d) Sanji, T.; Nakatsuka, Y.; Ohnishi, S.; Sakurai, H. *Macromolecules* **2000**, *33*, 8524. (e) Hartgerink, J. D.; Beniash, E.; Stupp, S. I. *Science* **2001**, *294*, 1684.
- (3) Moore, J. S. *Acc. Chem. Res.* **1997**, *30*, 402.
- (4) Grayson, S. M.; Fréchet, J. M. J. *Chem. Rev.* **2001**, *101* (12), 3819.

- (5) (a) Knolker, H. J.; Reddy, K. R. *Chem. Rev.* **2002**, *102* (11), 4303. (b) Kawde, R. B.; Santhanam, K. S. V. *Bioelectrochem. Bioenerg.* **1995**, *38*, 405. (c) Annie, D. B.; Dubois, J. E.; Lacaze, P. C. *J. Electroanal. Chem.* **1985**, *189*, 51.
- (6) (a) Miller, J. S. *Extended Linear Chain Compounds*; Plenum: New York, 1983; Vol. 1–3. (b) Metzger, R. M.; Day, P.; Papavassiliou, G. C. *Lower-Dimensional Systems and Molecular Electronics*; Plenum Press: New York, 1990.
- (7) (a) Ball, P. *Nature* **1996**, *383*, 561. (b) Morteani, A. C.; Dhoot, A. S.; Kim, J.-S.; Silva, C.; Greenham, N. C.; Murphy, C.; Moons, E.; Cina, S.; Burroughes, J. H.; Friend, R. H. *Adv. Mater.* **2003**, *15*, 1708. (c) Chen, X. L.; Jenekhe, S. A. *Macromolecules* **1996**, *29*, 6189.
- (8) (a) Taranekar, P.; Fan, X.; Advincula, R. *Langmuir* **2002**, *18* (21), 7943. (b) Taranekar, P.; Baba, A.; Fulghum, T. M.; Advincula, R. *Macromolecules* **2005**, *38*, 3679. (c) Inaoka, S.; Roitman, D. B.; Advincula, R. C. *Chem. Mater.* **2005**, *17* (26), 6781.

Scheme 1. Synthesis of G1 and G2 Dendrons



sonication mediated synthetic route which led to high yielding and faster synthesis results. To our knowledge this is the first attempt to synthesize Fréchet type dendrons and dendrimers using a sonication method. Sonication⁹ and microwave¹⁰ methods have long been employed for enhancing the rate of chemical reactions. For better efficiency, microwave-assisted synthesis is often performed without solvents, making this method not ideally compatible for syntheses involving molecules with high molecular weight or low solubility, as in the case of dendrimer synthesis. Sonication, on the other hand, may provide the needed energy (acoustic and thermal) to overcome the different reactivities and enable the development of general protocols for facilitating the synthesis of dendrons and dendrimers. In this work, we demonstrate the use of sonication methods in a Mitsunobu reaction, which involves both etherification and esterification reactions in solution to obtain the desired dendrons and dendrimers in sufficiently high yield. Conventionally, a reaction time of 3–4 days is required to achieve synthetically useful yields (70–75%). But under the present reaction conditions and submitted to sonication conditions, we obtained comparative yields in only 2–4 h.

We specifically targeted these carbazole jacketed precursor dendrimers for several reasons: (i) the carbazole group is one of the most attractive chromophores in photochemistry and has been extensively studied;¹¹ (ii) the carbazole groups act as good hole transport materials for LED devices; and last (iii), the carbazole group is electrochemically active forming insoluble polycarbazole polymers based on 3,6 or 2,7 reactivity as a film on the desired substrate.¹² It is well-known that Poly(*N*-vinylcarbazole) (PVK) is a good photoconductor, whereas

monomers such as *N*-ethylcarbazole and *N*-propylcarbazole are poor photoconductors.¹³ Therefore, another purpose of this work is to investigate the unique optoelectronic properties and electropolymerizability phenomena by cross-linking peripheral carbazole moieties as a function of dendrimeric generations that would be significantly different from its linear polymer counterpart, i.e., PVK. Although previously some groups have reported dendrimers containing peripheral electropolymerizable groups with thiophenes,¹⁴ the ultimate structure–property relationship in a generational dendrimeric system remains highly unexplored. In the past, we have used a linear “precursor polymer” route to form conjugated network films of these polycarbazoles which can be deposited and patterned by electrochemical methods.¹⁵ A series of generational precursors were synthesized, which by design contained the peripheral electroactive carbazole monomer units.

The polyether possesses a low T_g and therefore in principle could undergo conformational changes as a function of generation, which then allows one to fine-tune the properties such as optical, electronic, morphological, and ion permeability within this series. Electropolymerization or chemical oxidation will result in a network conjugated polymer having both inter- and intramolecular cross-linking possibilities. Thus in this report, we present a design and synthesis strategy using sonication chemistry and a detailed insight into the structure–property relationship as a function of generation for a series of carbazole terminated polybenzylether dendrimers.

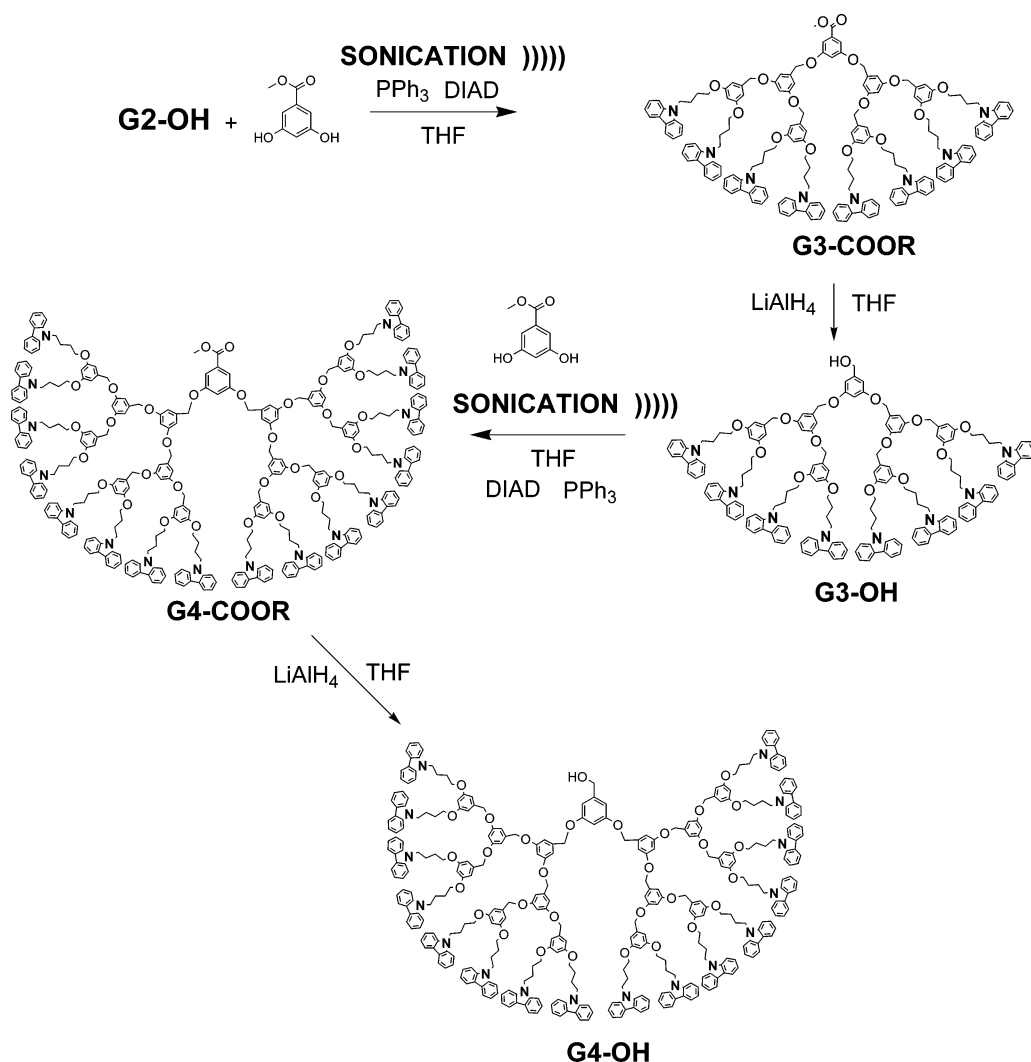
Results and Discussion

Structural Design and Synthesis. The synthetic routes for the generation one (G1) and two (G2) carbazole terminated dendrons are shown in Scheme 1. The synthesis was started using carbazole and 1,4-dibromobutane to produce 9-(4-bromobutyl)-9H-carbazole (CBZ-Br) in a modified procedure used previously by Shen et al.^{11a}

- (9) (a) Lepore, S. D.; He, Y. *J. Org. Chem.* **2003**, *68*, 8261. (b) Gholap, A. R.; Venkatesan, K.; Daniel, T.; Lahoti, R. J.; Srinivasan, K. V. *Green Chem.* **2003**, *6*, 693. (c) Chen, M.-Y.; Lu, K.-C.; Lee, A. S.-Y.; Lin, C.-C. *Tetrahedron Lett.* **2002**, *43*, 2777.
- (10) Tierney, J. P.; Lidstrom, P. *Microwave Assisted Organic Synthesis*; Blackwell Publishing: Oxford, U.K., 2005; Vol. 280, p 89.
- (11) (a) Bo, Z.; Zhang, W.; Zhang, X.; Zhang, C.; Shen *J. Macromol. Chem. Phys.* **1998**, *199* (7), 1323. (b) Zhu, Z.; Moore, J. S. *Macromolecules* **2000**, *33*, 801. (c) Kimoto, A.; Cho, J. S.; Higuchi, M.; Yamamoto, K. *Macromolecules* **2004**, *37*, 5531. (d) Fu, Y.; Li, Y.; Li, J.; Yan, S.; Bo, Z. *Macromolecules* **2004**, *37*, 6395. (e) Romero, D. B.; Schaer, M.; Leclerc, M.; Ades, D.; Siove, A.; Zuppiroli, L. *Synth. Met.* **1996**, *80*, 271.
- (12) (a) Liu, X.-M.; Xu, J.; Lu, X.; He, C. *Org. Lett.* **2005**, *7* (14), 2829. (b) Li, J.; Liu, D.; Li, Y.; Lee, C.-S.; Kwong, H.-L.; Lee, S. *Chem. Mater.* **2005**, *17* (5), 1208.

- (13) Ostroverkhova, O.; Moerner, W. E. *Chem. Rev.* **2004**, *104* (7), 3267.
- (14) (a) Sebastian, R.; Caminade, A.; Majoral, J.; Levillain, E.; Huchet, L.; Roncali, J. *Chem. Commun.* **2000**, 507. (b) Alvarez, J.; Sun, L.; Crooks, R. M. *Chem. Mater.* **2002**, *14* (9), 3995.
- (15) (a) Taranekar, P.; Baba, A.; Fulghum, T. M.; Advincula, R. *Macromolecules* **2005**, *38* (9), 3679. (b) Taranekar, P.; Fulghum, T. M.; Baba, A.; Patton, D.; Advincula, R. *Langmuir* **2007**, *23*, 908.

Scheme 2. Synthesis of G3 and G4 Dendrons



Similarly, we have also modified the synthesis of (G1) dendron ester (G1-COOR) reported earlier by Bo et al.^{11d} in a synthetically useful yield of 70%. The purification of G1-COOR does not require any column chromatography. It can be easily purified by recrystallization using ethyl acetate.

The G1-COOR was then reduced using lithium aluminum hydride (LAH) to produce the G1 dendron alcohol (G1-OH) in 90% yield. The G1-OH dendron was then dissolved in minimal THF along with PPh₃ and methyl 3,5-dihydroxybenzoate, and DIAD was slowly added under sonication conditions to produce G2-COOR in 84% yield within 75 min (Caution: Water in the sonicator turns very hot if used for prolonged periods of time). The amount of THF is very important. It should only be used to barely dissolve the starting alcohol. Excess THF, temperature fluctuations in the sonication bath, and scaling above 6 g caused a significant lowering in the yields. The G2-COOR was further reduced to G2-OH.

The synthesis protocol of generation three (G3) dendrons is shown in Scheme 2. The G3-COOR was prepared by sonication using G2-OH and once again under sonication for 3 h to afford a white solid product in 70.8% yield after purification. The G3-COOR was also eventually converted to G3-OH using LAH in 85% yield. The G3-OH was coupled with methyl 3,5-dihydroxybenzoate using sonication conditions to produce G4-

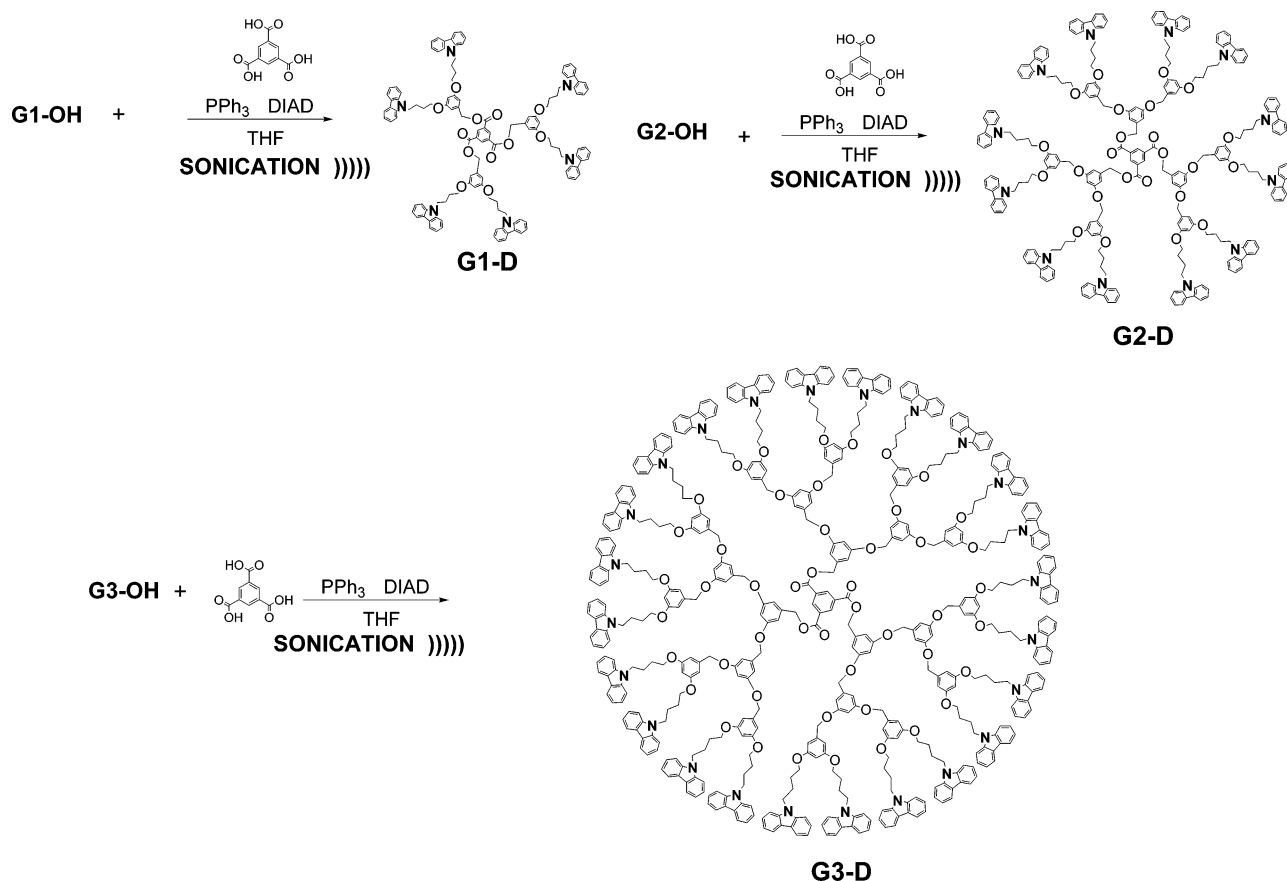
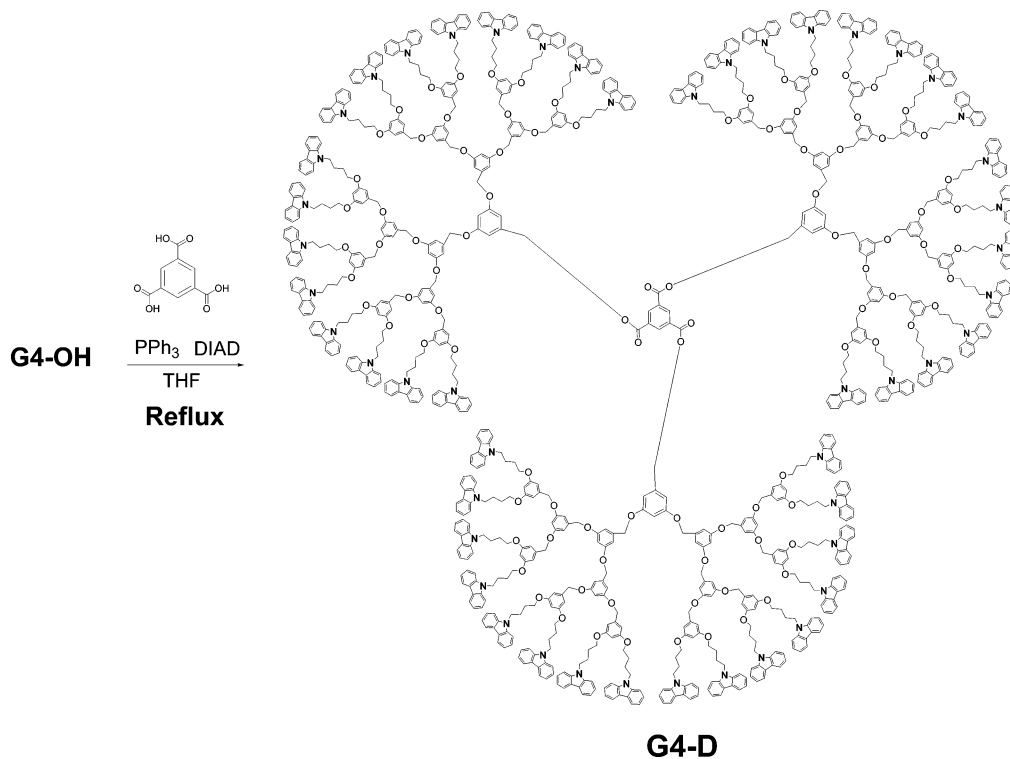
COOR as shown in Scheme 2. It took 4 h to obtain a synthetically useful yield of 68.6%, which on the other hand took 5 days under stirring conditions to produce comparable yields. The G4-COOR was then further reduced to G4-OH in 81% yield.

Direct coupling of these dendrons afforded the dendrimer structures (Schemes 3 and 4). Compound G_x-OH (*x* = 1, 2, 3, 4) was coupled with benzene-1,3,5-tricarboxylic acid (BTC) as a core using Mitsunobu esterification, again under sonication. BTC was purposely used as a core so that we can potentially extend the expansion of applications for these dendrimers. Recently we have demonstrated that these dendrimers can be intramolecularly cross-linked both chemically and electrochemically.¹⁶

However, even after several repeated trials under sonication with varying concentration or even prolonged time, disubstituted product was isolated. Finally, under refluxing for 6 days and under similar chemical conditions all three dendrons were successfully grafted to the core yielding G4-D in 51% yield as shown in Scheme 4.

Characterization of Dendrimers. The dendrimers were found to be highly soluble in common organic solvents such as

(16) Taranekar, P.; Park, J.-Y.; Fulghum, T.; Patton, D.; Advincula, R. *Adv. Mater.* **2006**, *18* (18), 2461.

Scheme 3. Synthesis of G1/G2/G3-Carbazole Terminated Dendrimers**Scheme 4.** Synthesis of G4-Carbazole Terminated Dendrimer

CHCl_3 , CH_2Cl_2 , and THF and insoluble in acetone and ethyl acetate. The synthesized dendrimers were characterized using NMR and elemental analysis. With increasing dendrimer generation, the ^1H and ^{13}C NMR signals become more com-

plicated and it is difficult to discern the structures. To assess more clearly the identity of the chemical structures, further characterization was performed using MALDI-TOF (Matrix assisted laser desorption ionization-time-of-flight) mass spec-

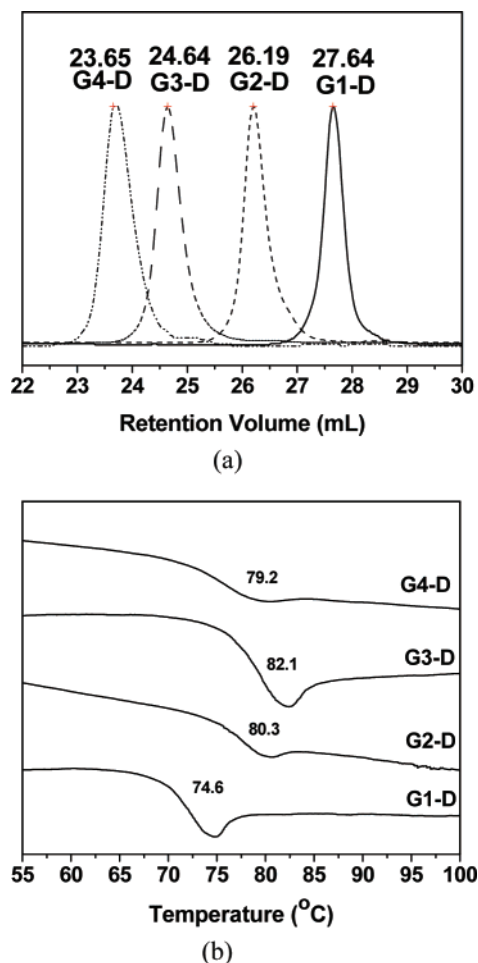


Figure 1. Characterization of dendrimers using (a) GPC chromatogram and (b) DSC.

troscopy. The sample was prepared by a method called “thin layer application” using *trans*-3-indoleacrylic acid (IAA) as a matrix. All generations of the dendrimers showed the corresponding ion peak of $M^+ + Na$ (Supporting Information Figure 1a).

The gel permeation chromatography (GPC) results are shown in Figure 1a. The retention volume trace and the polydispersity were found to be less than 1.02. The elution curves were found to be narrow and monomodal in distribution. Furthermore, a decreasing trend in the differences of retention volume was observed in going from lowest generation to the highest. The difference increases in going from G1-D to G2-D > G2-D to G3-D \gg G3-D to G4-D, which indicates that the hydrodynamic volume drastically changes after the third generation. This is reasonable as the higher generation dendrimer behaves much more like a large macromolecule with the exponential growth of branching.

The thermal properties of the dendrimers were investigated using differential scanning calorimetry (DSC) as shown in Figure 1b. The DSC traces of the second heating cycle (10 °C/min) showed glass transition temperature (T_g) values of 74.6, 80.3, 82.1, and 79.2 °C corresponding to G1-D, G2-D, G3-D, and G4-D, respectively. Interestingly, the G4-D dendrimer falls off the increasing trend of T_g , suggesting that there is a huge structural change consistent with the observed hydrodynamic specific volume in GPC. Thus, we believe that this change

reinforces the fact that the G4-D dendrimer structurally rearranges and creates a dense phase resulting in more intermolecular interactions within the macromolecule. In this case a much higher degree of branching results in a lowering of the T_g , perhaps due to a higher benzylether content compared to the carbazole.^{11a} This unique behavior can only be expected from dendrimers and not linear polymers. A low T_g value can be highly desirable with a higher generation as it could in principle lead to interesting optoelectronic trends correlated with viscoelastic behavior.

Thermogravimetric analysis (TGA) studies reveal that all the dendrimers except G1-D showed almost similar TGA onsets indicating a relatively high thermal stability compared to that for G1-D (Supporting Information Figure 1b). The ester groups are more vulnerable in the case of G1-D, and the initial mass loss was found to be equal to that of three CO₂ groups, which indicated the degradation of ester groups linked to the core. The thermal degradation onset of G1-D starts at 336 °C, while the higher generation dendrimers were found to be stable up to 375 °C. This is rational because, with increasing generations, the ester groups are more shielded and therefore the degradation occurs at higher temperatures.

Electrochemical/Morphological Studies. The different CV traces for all the generations of dendrimers are shown in Figure 2. The peak anodic and cathodic currents and potentials are summarized in Table 1. The CV for G1-D shows an unusually sharp reversible redox peak behavior as compared to the conventional CV behavior of polycarbazole (Figure 2a).¹⁷ The sharp reversible redox behavior could be attributed to either a very thin film, which in principle will show a homogeneous electron-transfer rate, or a dominance of electron transfer from either inter- or intramolecular species formed during cross-linking (higher conjugated units) or a combination of both. As a consequence, this material showed very fast doping–dedoping characteristics among the different generations.

The dendrimers G2-D and G3-D, compared to G1-D and G4-D, both show higher peak E_{pa} values. This clearly suggests that there is an optimal conformational freedom required to allow extended conjugation during cross-linking for these dendrimers. This could also possibly lead to 3,6 and 2,7 type cross-linking in the dendrimers. The presence of a small reduction peak at 1.05 is indicative of some 2,7^{18a} cross-linking, but the majority of cross-linking still occurs via the 3,6-position^{18b} as indicated by strong reduction peaks observed between 0.6 and 0.7 V. Although we did not observe any sharp redox peaks for the other generations, the CV behavior is still very different compared to that for the linear polycarbazole based polymer (PVK) (Supporting Information Figure 5) as evident by the shape and peak positions.^{18c} The fact that both G2-D and G3-D show a higher ΔE ($E_{pa} - E_{pc}$) value shown in Table 1 indicates a more heterogeneous and slow electron-transfer rate for these two. This heterogeneous electron transfer is also likely a consequence of a thicker film deposited during each CV cycle and is also indicative of a higher cross-linking.

- (17) (a) Ambrose, Nelson *J. Electrochem. Soc.* **1968**, *115*, 1159. (b) Kakuta, T.; Shirota, Y.; Mikawa, H. *J. Chem. Soc., Chem. Commun.* **1985**, 553. (c) Shirota, Y.; Nogami, T.; Noma, N.; Kakuta, T.; Saito, H. *Synth. Met.* **1991**, *41*, 1169.
- (18) (a) Iraqi, A.; Wataru, I. *Chem. Mater.* **2004**, *16* (3), 442. (b) Iraqi, A.; Pickup, D. F.; Yi, H. *Chem. Mater.* **2006**, *18* (4), 1007. (c) Fulghum, T.; Karim, S. M. A.; Baba, A.; Taranehar, P.; Nakai, T.; Masuda, T.; Advincula, R. C. *Macromolecules* **2006**, *39* (4), 1467.

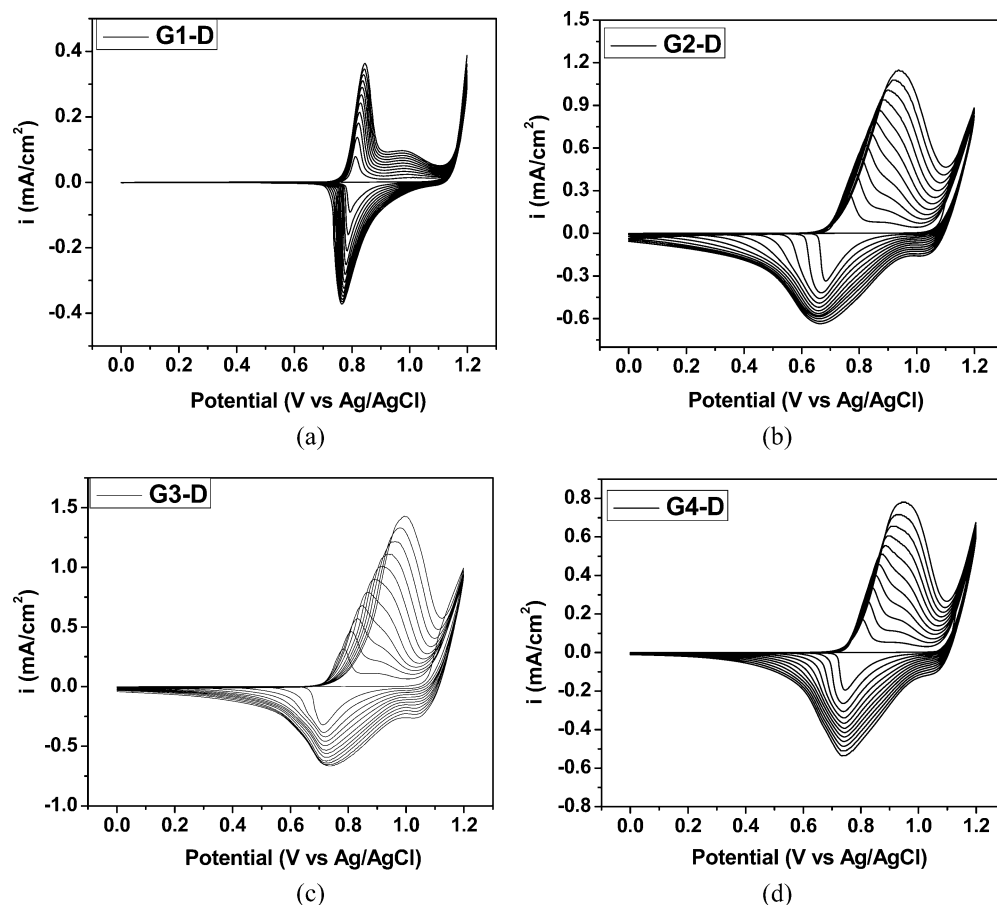


Figure 2. Cyclic voltammograms: (a) G1-D, (b) G2-D, (c) G3-D, (d) G4-D dendrimers.

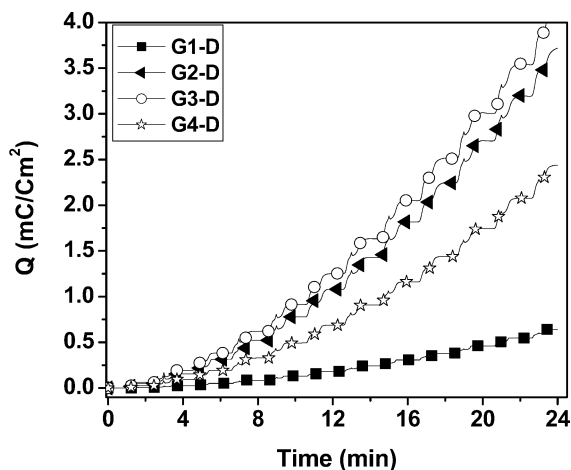


Figure 3. Amount of charge per unit area as a function of time during cross-linking.

The CV result also suggests that raising the G_n -D ($n = 1, 2, 3, 4$) generation increases the amount of longer conjugated segments in the cross-linked dendrimer. Such an evolution of the polymer structure could be related to the increasing probability of inter- and/or intradendrimer coupling of the carbazole units as the G_n -D augments. Thus, on going from G1-D to G4-D, the cross-linking shows interesting trends subjected to steric hindrance and the competitive nature of inter-/intradendrimer linkages. It is expected that a higher content of intramolecular linkages with higher G_n -D should also limit intermolecular steric interactions in forming a polycarbazole

chain structure. Consequently, effective conjugation would approach a hypothetical limit determined by the conformational restrictions and connectivity imposed by the underlying dendritic scaffold. In the present case, the limit seemed to be observed for the G4-D dendrimer and is predicted to show predominantly intramolecular cross-linking unlike the case in both G2-D and G3-D. A decrease in the intermolecular interactions is indicative of a decreasing capacitive behavior in these materials and is attributed to a drop in electronic conductivity as observed. Thus, the high thickness (as obtained by profilometry, Supporting Information Figure 2) and relatively low intermolecular interactions for G4-D (Figure 1d and Table 1) suggested a poorly cross-linked film.

The high thickness and poor cross-linking behavior also result in a less dense film. Another way to confirm this property is to obtain the ratio of charge (Q) to the thickness of the electrodeposited film during electrochemical cross-linking by CV under similar conditions as those seen in Figure 3. The electropolymerization efficiency is expressed by the ratio Q_{\max}/T (where Q_{\max} is the maximum amount of charge reversibly exchanged upon cycling and T is the total thickness of the film).

While an increase in the doping level of the polymer cannot be totally excluded, these results strongly suggest greater electropolymerization efficiency for G2-D/G3-D as 0.65%/0.61% and for G1-D/G4-D as 0.59%/0.35%, respectively. This phenomenon could reflect the increasing proximity of the intermolecularly polymerizable carbazole groups and was found to be highest in the case of G2-D and lowest for G4-D cross-linked dendrimer films. These results clearly suggest that both

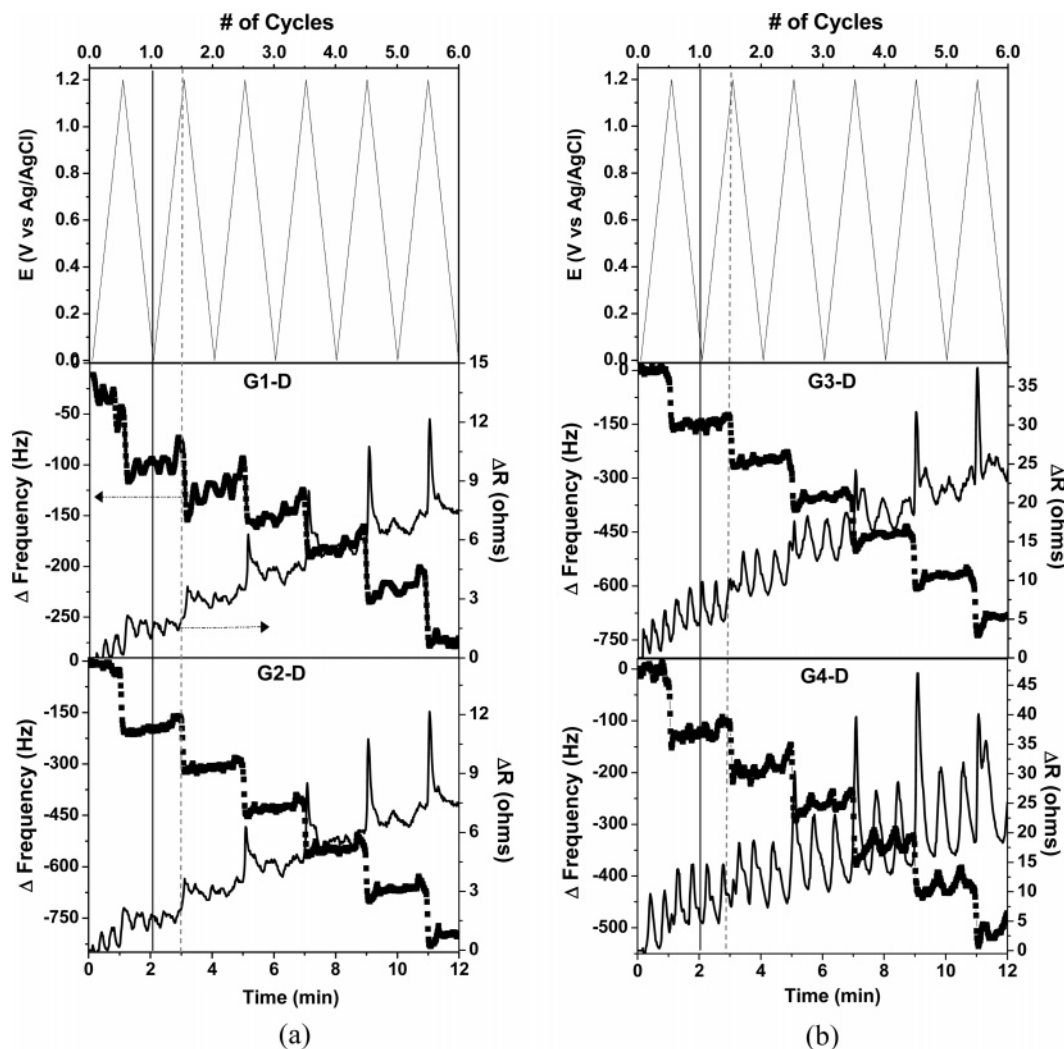


Figure 4. EC-QCM studies showing frequency and viscoelastic changes as a function of time for (a) G1-D, G2-D and (b) G3-D, G4-D.

Table 1. Dendrimeric Precursors Showing Peak Anodic and Cathodic Currents/Potentials and Their Corresponding Onsets of Oxidation Potential

dendrimers	onsets	E_{pa} (V)	i_p (mA)	E_{pc} (V)	i_{pc} (mA)	ΔE (V)	thickness (nm)
G1-D	0.99	0.84	0.35	0.76	-0.36	0.08	98.5
G2-D	0.94	0.93	1.14	0.67	-0.64	0.26	534.7
G3-D	0.95	0.99	1.42	0.72	-0.65	0.27	636.8
G4-D	1.03	0.94	0.77	0.74	-0.53	0.20	651.1

dendrimers G2-D and G3-D are good candidates for forming uniform and highly dense polycarbazole films on the conducting substrate. This study has demonstrated that confirmation and connectivity (branching topology) play a huge role when depositing to form a cross-linked conjugated polymer film. The fact that one can have facile control of the inter/intramolecular cross-linking with the use of dendrimers could potentially lead to more interesting electro-optical property variations. Finally, all cross-linked films formed were optically clear and uniform and therefore could be envisioned as potential candidates for OLED and other display device applications.

In an attempt to understand the electron-transfer kinetics in the generational films, we have also performed CV in “monomer free” or electrolyte solution conditions at a scan rate of 25, 50, 100, and 200 mV/s in methylene chloride solution containing 0.1 mM tetrabutylammonium hexafluorophosphate [TBAP]

(Supporting Information Figure 3). The linear increase of i_{pa} as a function of scan rate with reversible redox peak indicates a more homogeneous electron transfer or ion transport rate as seen from Supporting Information Figure 3a for the case of G1-D. In G2-D, G3-D, and G4-D, we did not observe linearity in the peak current as a function of scan rate, which indicates more heterogeneous and diffusion-limited electron-transfer kinetics for these films. For instance, if the electronic transfer at the surface is fast and the current is limited by the diffusion of species to the electrode surface, then the current peak will be proportional to the square root of the scan rate. The diffusion-limited kinetics could result from the highly branched topology and dendrimeric conformational changes influencing the film morphology ion porosity and electron-transfer kinetics. This could also be attributed to an increased distance between the solution/film interface and the electrode or in other words the higher thickness of the film with increasing G_n -D. Two-dimensional (2D) and three-dimensional (3D) atomic force microscopy images were also investigated for the cross-linked films (Supporting Information Figure 4). Although it is hard to distinguish any marked differences between the cross-linked films, sharp conical features and uniform surface coverage seemed to be a function of the extent of cross-linking. The root-mean-square roughness (rms) of the dendrimers G1-D, G2-D,

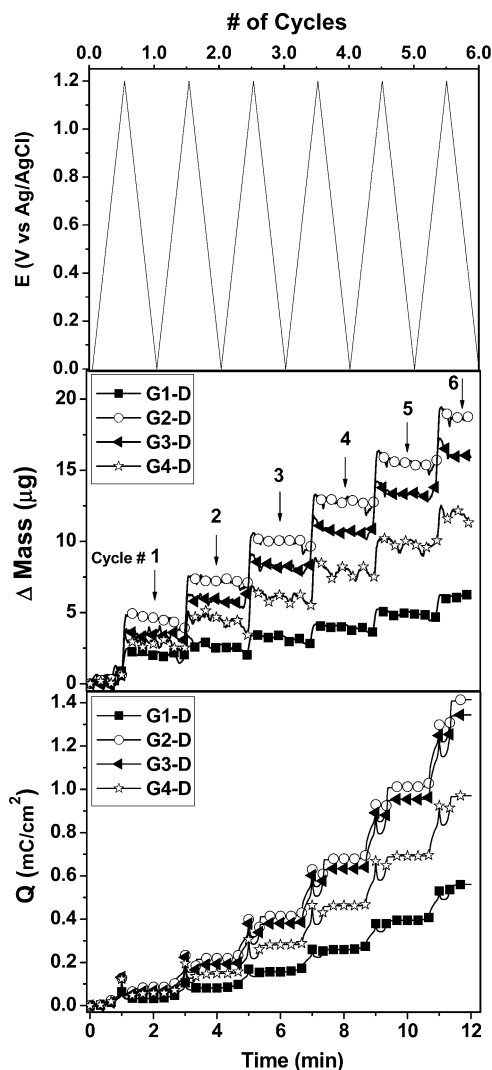


Figure 5. EC-QCM: Amount of charge and simultaneous mass deposition as a function of time.

G3-D and G4-D were found to be 1.25, 0.756, 1.04, and 1.2 nm, respectively.

In Situ EC-QCM Studies. Electrochromism is another possible application of these materials and therefore relies highly on doping–dedoping characteristics, and in order to fully understand the cross-linking process and film densification, *in situ* electrochemical-quartz crystal microbalance (EC-QCM) analysis was performed. EC-QCM is an exceptionally versatile technique for *in situ* monitoring of gravimetric changes occurring at electrode surfaces.^{19a,b} The change in mass (Δm) is related to the change in the fundamental resonance frequency ΔF (Hz) of the QCM crystal by the well-known Sauerbrey equation (eq 1):^{19c}

$$\Delta F = \frac{-2F_q^2}{A_e \sqrt{\rho_q \mu_q}} \Delta m \quad (1)$$

where F_q is the fundamental resonant frequency of the QCM (5 MHz), A_e is the area of the electrode (1.327 cm²), ρ_q is the

density of the quartz (2.65 g/cm³), and μ_q is the shear modulus of the quartz (2.95 × 10⁶ N/cm²). This model equation is only valid if the adsorbed film thickness is small in comparison with the thickness of the crystal and if the ΔF is much smaller than the resonant frequency of the bare crystal. Furthermore, the mass sensitivity has previously been shown to be approximately the same for liquid and air/vacuum measurements yielding the ability to accurately monitor changes in mass adsorbed from solution.²⁰ However, an adsorbed viscoelastic overlayer in the case of viscous liquids and some polymer thin films result in a viscous coupling of the solution or film to the crystal, effectively adding a mass component to the oscillating crystal. Thus, the resulting resonant frequency change is more complex and was first described by Kanazawa et al. as follows (eq 2):²⁰

$$\Delta F = -f_q^{3/2} \sqrt{\frac{\eta_L \cdot \rho_L}{\pi \cdot \mu_q \cdot \rho_q}} \quad (2)$$

where f_q is the resonant frequency of unloaded crystal in Hz; ρ_q is the density of quartz (2.648 × 10³ kg/m³); μ_q is the shear modulus of quartz (2.947 × 10¹⁰ Pa); ρ_L is the liquid density kg/m³; and η_L is the liquid viscosity in contact with electrode in N s/m². Hence, when the QCM operates under inelastic conditions, it becomes difficult to differentiate contributions attributed to the bound mass from that of the solution viscosity to the total change in frequency (ΔF).^{21a} In the present case using dendrimeric precursors, this factor becomes very important, since the solvent could essentially penetrate in the voids that are present in the dendrimers especially with the higher generation (G3-D/G4-D).

In this case, impedance analysis of the QCM resonator has proven to be effective in providing additional information on the solid/liquid interface.^{21b} This analysis is based on the well-known Butterworth–van Dyke (B–VD) equivalent circuit which provides the structure for relating the electrical properties of the quartz resonator to the mechanical properties of the deposited film.

In this regard, the B–VD circuit element R (motional resistance) is useful in probing the energy loss or dissipation factor (D) due to the damping process which occurs in viscoelastic systems.²² Thus, an increase in ΔR is correlated with an increase in the viscoelasticity of the layer adjacent to the crystal surface while a small change in ΔR is indicative of a more rigid adsorbed layer. So, monitoring the change in the resonance resistance (ΔR (Ω)) as a function of frequency shift, in some cases, provides a means for quantitatively determining the shear viscosity and elastic modulus of films and in others a means for qualitatively comparing various thin film systems. Here, E-QCM was performed to simultaneously monitor the change in mass and resonance resistance at the working electrode during the electrochemical deposition of the dendrimer precursors. CV was utilized to study the electrochemical behavior of the carbazole-modified dendrimers as deposited from solution. ΔF changes in resonance resistance (ΔR) as a function of time during cyclic voltammograms (CVs) of various generation dendrimers deposited from a 0.1 M TBAP/CH₂Cl₂ (scan rate 20 mV s⁻¹) solution (Figure 4). Increasing ΔF changes

(19) (a) Abruña, H. D. *Electrochemical Interfaces: Modern Techniques for In situ Interface Characterization*; VCH Publishers: New York, 1991. (b) Buttry, D. A.; Ward, M. D. *Chem. Rev.* **1992**, *92*, 1355. (c) Sauerbrey, G. *Z. Phys.* **1959**, *155*, 206.

(20) Kanazawa, K. *Faraday Discuss.* **1997**, *107*, 77.

(21) (a) Ward, M. D.; Buttry, D. A. *Science* **1990**, *249*, 1000. (b) Etchenique, R.; Weisz, A. *J. Appl. Phys.* **1999**, *86*, 1994.

(22) Muramatsu, H.; Tamiya, E.; Karube, I. *Anal. Chem.* **1988**, *60*, 2142.

indicates the deposition of G1-D dendrimer as a film up to six cycles (Figure 4a). The dotted line represents the frequency shift during a second CV cycle starting over the potential range for the oxidation (1.1–1.2 V, anodic scan) and reduction (1.0–0.7 V, cathodic scan) of the polycarbazole formation and is indicative of the deposition of a thin film. Simultaneously, ΔR values were recorded during each CV cycle, which indicates the change in the viscoelastic behavior. As seen from Figure 4a, initially the ΔR is small, but from the third cycle the change becomes apparent showing considerable doping–dedoping changes due to a thicker film.

On the other hand G2-D compared to G1-D shows a relatively huge ΔF change, which indicates more mass deposition that could be due to the higher extent of cross-linking and favorable conformational changes. However, the ΔR values remain unchanged, which indicates a more densely packed film. This may be attributed to a decrease in free volume within the G2-D thin film, which would result in a more rigid mechanical response. Figure 4b shows a similar complex stepwise response in frequency and resonance resistance for G3-D and G4-D with each potential cycle indicating processes related to the deposition, doping, and dedoping of the polymer film. In the anodic scan, the doping occurs at 0.6 V and one expects to observe a decrease in ΔF , but we observed rather an opposite behavior. This could possibly be due to a relatively higher change in ΔF because of solvent expulsion rather than doping in the depositing film.

With increasing CV cycles, the ΔF and particularly the ΔR response resulting from the deposition, doping, and dedoping processes becomes more prominent in the case of G3-D and G4-D as compared to lower generations. A higher ΔR value as compared to the lower generation indicates a more viscoelastic film. In the case of G4-D, due to the conformational and structural restraints a poor cross-linking occurs, which is reflected in the highest ΔR change as compared to any other case. This indicates that a poorly cross-linked film in the case of G4-D also has a very low density.

The mass of the polymer depositing on the working electrode was found to be linear as a function of the CV cycle, and a corresponding increase in the amount of charge is indicative of the extent of cross-linking in an electrochemically active thin film as shown in Figure 5. The change in mass remains constant for the anodic scan up to a potential of 0.6 V. At this point, the onset of mass transport was observed with a sharp increase from 0.65 V, which is correlated to the injection of anions into the film upon doping. This is supported by the simultaneous increase in charge over this potential range. A second regime of mass change was observed from ~ 1.1 to 1.2 V in the anodic scan and from 1.2 to 1.1 V in the cathodic scan which is mostly due to the oxidation of the peripheral-carbazole monomers or growing carbazole chain radical to form a more conjugated polymer network. On the other hand, the overall increase in mass is a combination of both doping and polymer deposition. The ejection of anions from the film (dedoping) was observed by a corresponding decrease in mass at potentials from ~ 0.8 to 0.5 V in the cathodic scan. Once again the polymerization efficiency calculated from the mass to charge ratio ($\Delta m/Q$) was found to be highest in the case of the G2-D dendrimer. These values are consistent with the previously calculated efficiency values during the CV discussion.

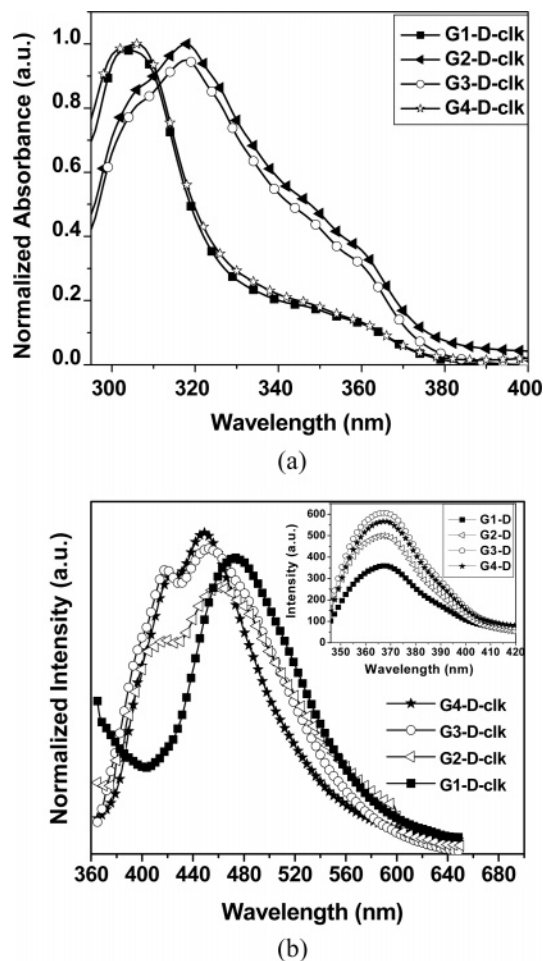


Figure 6. Optical studies of dendrimers: (a) UV–vis spectra and (b) photoluminescence.

Absorption and Photoluminescence Studies. The cross-linked films were further characterized by studying their optical properties. The UV–vis spectra of the cross-linked films are shown in Figure 6a. The extent of increasing π orbital overlap between neighboring repeat units on conjugated polymers can be directly assessed from their electronic spectra. The extent of electronic conjugation directly affects the observed energy of the π – π^* transition, which appears as the absorption maxima in these materials. This could be due to the possibility of either inter/intramolecular cross-linking dominating the π – π^* transition. The values of absorption maxima for the different generations are closely linked to their degree of polymerization. As seen from Figure 6a, both G1-D and G4-D reveal a λ_{max} value between 308 and 310 nm.

These values are similar to the absorption maxima of 9-alkyl-9H-carbazole dimers and indicate a restriction of electronic conjugation along polymer chains in this series to about two carbazole rings, regardless of the huge conformation and branching topology difference between both dendrimers. This data seem to be consistent with the CV trends, which shows a limited cross-linking in both dendrimers. On the other hand both G2-D and G3-D show a more red-shifted absorption value in the range 322–325 nm, indicating an extended conjugation. This could be due to the higher extent of intermolecular cross-linking within these dendrimers consistent with the CV data. The band gap of these materials, which are estimated from the onset of the absorption peak, lies in the range 3.3 to 3.2 eV, which

possibly indicates the presence of both 3,6- and 2,7-linkages in the conjugated polycarbazole network.¹⁸

The photoluminescence studies of un-cross-linked dendrimers performed in methylene chloride solution gave a λ_{max} at 365 nm (Figure 6b inset). The photoluminescence intensity due to the un-cross-linked peripheral carbazole increases with increasing generations, except in the case of G4-D. This could be due to inter/intramolecular self-quenching of the carbazole groups (aggregation), since this dendrimer has more carbazole groups at the periphery. The results of the photoluminescence of the cross-linked films are rather more interesting as seen from Figure 6b. For the G1-D-clk film the photoluminescence peak appears at a longer wavelength (474 nm) as compared to those for all the other dendrimers. The peak shows relatively sharp vibronic bands and appears to have the highest Stokes shift, indicating a large difference in the ground and excited state. The unique nature and highest red shift in the case of G1-D indicate a total dominance of one type of cross-linking (perhaps more intermolecular). The photoluminescence spectra of G2-D-clk shows a shoulder peak at 412 nm, and its major peak appears at 460 nm. The shoulder peak was also observed in G3-D-clk and G4-D-clk films. The major intensity peak for G3-D-clk and G4-D-clk films was found at 453 and 447 nm, respectively.

Band Gap Studies. In order to determine the band gap of these materials, we performed CV on the cross-linked films using 0.1 mM TBAP as a supporting electrolyte in methylene chloride and a saturated Ag/AgCl reference electrode (having a potential of 0.2 V versus NHE) was used. All polymers showed reversible oxidative behavior (Supporting Information Figure 6). Supporting Information Figure 6 insets show the oxidation onset (E_{onset}) during the anodic scan, which allows us to estimate the HOMO level within these materials. The measured oxidation potentials can be converted into ionization potentials by relating the electrochemical energy scale (with respect to NHE) to the vacuum energy scale. At room temperature, the Fermi level of NHE is -4.5 eV with respect to the vacuum level,²³ which means that the ionization potential (IP) can be calculated using $\text{IP [eV]} = 4.7 + E_{\text{onset}}$. The ionization potential can be taken as a measure of the energy of the highest occupied molecular orbital (HOMO). All the dendrimers displayed reversible oxidation peaks. The oxidizability of the dendrimers did not show any regular trend as a function of generation number. The HOMO level of G1-D, G2-D, G3-D, and G4-D were found to be -5.4 , -5.2 , -5.3 , and -5.4 eV. For the present case the highest HOMO (-5.2 eV) value was found for G2-D and, accordingly, is expected to have the lowest barrier to hole injection. The LUMO level was estimated from the onset of the UV-vis and was found to be -2.09 , -1.97 , -2.03 , and -2.12 corresponding to G1-D, G2-D, G3-D, and G4-D, respectively. The LUMO level of G2-D is close to the LUMO level of PVK (-1.8 eV), but the HOMO level of G2-D (-5.2 eV) is far superior to its linear polymer analogue PVK (-5.9 eV).²⁴

Conclusion

In summary, benzyl ether based carbazole terminated dendrons and dendrimers up to generation four have been successfully synthesized by Mitsunobu coupling under sonication conditions. All the characterization results including NMR, elemental analysis, GPC, and MALDI-TOF confirmed the structures as proposed in the schemes. The electrochemical cross-linking of the dendrimers as thin films revealed unusual CV behavior depending upon the generations. G1-D showed a higher extent of intermolecular cross-linking while G4-D showed a higher extent of intramolecular cross-linking. On the other hand, G2-D and G3-D tend to form a better balance between intra- and intermolecular cross-linking resulting in dense and more electrochemically active films. The cross-linked dendrimers were found to show a diffusion controlled kinetic behavior for all the generations except G1-D. The fluorescence of G1-D compared to other dendrimers was found to be red-shifted. The EC-QCM results confirmed that both G2-D and G3-D show efficient deposition and cross-linking behavior. The G4-D dendrimer shows the highest viscoelastic change during film formation. A tunable HOMO level and optically clear films were formed from these dendrimers making them very suitable and promising candidates for future LED device applications and materials for nanoscience. These materials are currently being systematically investigated for their optical, electronic, and conformation dependent band gap variation for improved hole transport and patterning in ultrathin films.

Experimental Section

Synthesis of 9-(4-Bromobutyl)-9H-carbazole [CBZ-Br] (Scheme 1). The synthesis of 9-(4-bromobutyl)-9H-carbazole was accomplished by a modified method as reported by Shen et al.^{11a} A mixture of 10.32 g (61.72 mmol) of carbazole in toluene (100 mL) containing 1,4-dibromobutane (118.2 g, 547.4 mmol) and tetrabutylammonium bromide (TBAB, 2 g) was stirred at 45 °C for 3 h and then left overnight. After the aqueous layer was removed and washed three times with water and brine, the organic layer was dried over Na_2SO_4 . The organic solvent was evaporated, and unreacted 1,4-dibromobutane was removed by vacuum distillation. The residue was recrystallized from ethanol to give 16.7 g (89.5%) of the product. The characterization was found to be consistent with the literature.

Synthesis of Methyl 3,5-Bis(4-(9H-carbazol-9-yl)butoxy)benzoate [G1-COOR] (Scheme 1). In a literature modified process as reported by Bo et al.,^{11d} a mixture of 15.22 g (50.37 mmol) of CBZ-Br, 21.0 g of K_2CO_3 , 3.94 g (23.4 mmol) of methyl 3,5-dihydroxybenzoate, 500 mL of acetone, and 45 mg of 18-crown-6 was stirred and refluxed under a nitrogen atmosphere for 72 h. Acetone was evaporated under vacuum, and the residue was partitioned between water (400 mL) and CH_2Cl_2 (500 mL). The organic layer was separated, and the aqueous layer was extracted three times with CH_2Cl_2 (250 mL). Finally, the combined organic layer was dried over Na_2SO_4 . After removal of the solvent, the residue was recrystallized from ethyl acetate to give a white solid product in 70% yield. The characterization data were found to be consistent with the literature.

General Method for Lithium Aluminum Hydride (LAH) Reduction of Aromatic Esters to Benzylic Alcohols (Method A). The aromatic ester was added dropwise to a suspension of LAH in THF cooled to 0 °C with an ice bath. The suspension was then allowed to warm to room temperature and was stirred until the reaction was complete as indicated by TLC. The reaction was quenched by adding water, and the THF was removed under reduced pressure in a rotary evaporator. The resulting layer was brought to a neutral pH with the addition of 2 N HCl solution and extracted with CH_2Cl_2 . The organic

(23) Bockris, J. O. M.; Khan, S. U. M. *Surface Electrochemistry. A Molecular Level Approach*; Kluwer Academic/Plenum Publishers: New York, 1993.

(24) van Dijken, A.; Bastiaansen, J. J. A. M.; Kiggen, N. M. M.; Langeveld, B. M. W.; Rothe, C.; Monkman, A.; Bach, I.; Stossel, P.; Brunner, K. J. *Am. Chem. Soc.* **2004**, *126* (24), 7718.

layers were combined, washed with water, dried over sodium sulfate, filtered, and concentrated under reduced pressure. The product was purified by silica gel flash column chromatography using a 20/4/1 CH₂-Cl₂/hexane/ethyl acetate eluent.

General Method for Etherification Reactions (Method B). The Mitsunobu etherification and esterification method was performed using sonication. The mixture of alcohol, phenol (or aromatic carboxylic acid), and triphenylphosphine (PPh₃) in *minimal* THF was cooled to 5 °C with an ice bath and sonicated for 5 min. Under sonication, a solution of diisopropyl azodicarboxylate (DIAD) was added dropwise under nitrogen. The water temperature was allowed to warm to room temperature, and precautions were taken to maintain the temperature. (Caution: Water in the sonicator turns very hot if sonicated for a long time.) Sonication was performed until the reaction was completed as indicated by TLC. The product was purified using 4/1 CH₂Cl₂/hexane as an eluent by silica gel column chromatography. *Note:* In the case of the G4-dendrimer (G4-D), sonication did not yield the desired product and therefore a reflux condition was used to obtain the final product. The product was purified using neutral alumina and a 6/1 ratio of CH₂-Cl₂/hexane.

Synthesis of (3,5-Bis(4-(9H-carbazol-9-yl)butoxy)phenyl)methanol [G1-OH] (Scheme 1). Following the general synthesis method A as described above, the reaction of 1.0 g (23.3 mmol) of LAH in 300 mL of THF with a solution of 9.5 g (15.5 mmol) of G1-COOR in 400 mL of THF afforded a white solid in 90% yield. ¹H NMR (CDCl₃): δ (ppm) 8.10 (d, 4H, *J* = 7.5 Hz), 7.53–7.42 (m, 8H), 7.25–7.22 (m, 4H), 6.45 (d, 2H, *J* = 2.1 Hz), 6.28 (t, 1H, *J* = 2.1 Hz), 4.59 (s, 2H), 4.39 (t, 4H, *J* = 6.9 Hz), 3.91 (t, 4H, *J* = 6.2 Hz), 2.02–2.12 (m, 4H), 1.87–1.78 (m, 4H). ¹³C NMR (CDCl₃): δ (ppm) 160.26, 144.33, 140.38, 128.4, 125.7, 122.89, 120.44, 118.89, 108.69, 105.19, 100.57, 67.58, 65.34, 42.75, 27.02, 25.91. Anal. Calcd: C, 80.38; H, 6.57; N, 4.81. Found: C, 80.12; H, 6.44; N, 4.95.

Synthesis of Methyl 3,5-Bis(3',5'-bis(4-(9H-carbazol-9-yl)butoxy)benzyloxy)benzoate [G2-COOR] (Scheme 1). Following the general synthesis for method B as described above, a precooled solution of 0.86 g (5.15 mmol) of methyl 3,5-dihydroxybenzoate, 6 g (10.3 mmol) of G1-OH, and 2.7 g (10.3 mmol) of PPh₃ in THF under sonication was treated with a solution of DIAD (2.08 g, 10.3 mmol) in 3 mL of THF under nitrogen. The solution was sonicated for 1.5 h to afford a white solid product in 84% yield after purification. ¹H NMR (CDCl₃): δ (ppm) 8.09 (d, 8H, *J* = 7.5 Hz), 7.48–7.39 (m, 16H), 7.27–7.21 (m, 8H), 7.19(d, 2H, *J* = 2.1 Hz), 6.76 (t, 1H, *J* = 2.1 Hz), 6.50 (d, 4H, *J* = 2.1 Hz), 6.31 (t, 2H, *J* = 2.1 Hz), 4.94 (s, 4H), 4.37 (t, 8H, *J* = 7.5 Hz), 3.91–3.87 (m, 11H), 2.08–2.03 (m, 8H), 1.85–1.78 (m, 8H). ¹³C NMR (CDCl₃): δ (ppm) 166.70, 160.22, 159.87, 140.32, 138.72, 132.02, 125.63, 122.84, 122.47, 120.38, 118.82, 110.03, 108.63, 108.33, 107.34, 105.82, 100.87, 70.11, 69.98, 67.98, 67.53, 52.27, 42.67, 26.93, 25.84, 25.62. Anal. Calcd: C, 79.60; H, 6.21; N, 4.32. Found: C, 79.53; H, 6.12; N, 4.60.

Synthesis of (3,5-Bis(3',5'-bis(4-(9H-carbazol-9-yl)butoxy)benzyloxy)phenyl)methanol [G2-OH] (Scheme 1). Following the general synthesis for method A as described above, the reaction of 0.2 g (5.5 mmol) of LAH in 100 mL of THF with a solution of 4.2 g (3.2 mmol) of G2-COOR in 25 mL THF afforded a white solid product in 90% yield. ¹H NMR (CDCl₃): δ (ppm) 8.15 (d, 8H, *J* = 7.5 Hz), 7.53–7.42 (m, 16H), 7.31–7.25 (m, 8H), 6.59 (d, 2H, *J* = 2.1 Hz), 6.50–6.52 (m, 5H), 6.32 (t, 2H, *J* = 2.1 Hz), 4.95 (s, 4H), 4.59 (s, 2H), 4.36 (t, 8H, *J* = 6.9 Hz), 3.88 (t, 8H, *J* = 5.7 Hz), 2.11–2.00 (m, 8H), 1.87–1.76 (m, 8H). ¹³C NMR (CDCl₃): δ (ppm) 160.25, 160.09, 143.39, 140.37, 139.2, 125.69, 122.88, 120.4, 118.86, 108.66, 105.84, 105.72, 101.33, 100.81, 69.98, 67.57, 65.3, 42.72, 26.96, 25.88. Anal. Calcd: C, 80.41; H, 6.35; N, 4.41. Found: C, 80.48; H, 6.30; N, 4.60.

Synthesis of Methyl 3,5-Bis(3',5'-bis(3'',5''-bis(4-(9H-carbazol-9-yl)butoxy)benzyloxy)benzyloxy)benzoate [G3-COOR] (Scheme 2). Following the general synthesis for method B as described above, a precooled solution of 0.15 g (0.9 mmol) of methyl 3,5-dihydroxyben-

zoate, 2.3 g (1.8 mmol) of G2-OH, and 0.5 g (1.9 mmol) of PPh₃ in THF under sonication was treated with a solution of DIAD (0.38 g, 1.9 mmol) in 1 mL of THF under nitrogen. The solution was sonicated for 3 h to afford a white solid product in 70.8% yield after purification. ¹H NMR (CDCl₃): δ (ppm) 8.09 (d, 16H, *J* = 7.5 Hz), 7.47–7.35 (m, 16H), 7.30 (d, 2H, *J* = 2.1 Hz), 7.25–7.20 (m, 16H), 6.78 (b, 1H), 6.69 (b, 4H), 6.59 (b, 2H), 6.51 (b, 8H), 6.31 (b, 4H), 4.97 (s, 4H), 4.92 (s, 12H), 4.30 (t, 16H, *J* = 7.5 Hz), 3.88–3.81 (m, 19H), 2.07–1.95 (m, 16H), 1.78–1.73 (m, 16H). ¹³C NMR (CDCl₃): δ (ppm) 166.60, 160.17, 160.04, 140.25, 138.99, 138.80, 132.00, 125.60, 122.77, 120.31, 118.79, 108.59, 108.27, 107.07, 106.36, 105.77, 101.60, 100.77, 70.04, 69.97, 67.43, 52.23, 42.55, 26.85, 25.74. Anal. Calcd: C, 80.03; H, 6.19; N, 4.19. Found: C, 79.97; H, 6.20; N, 4.28.

Synthesis of (3,5-Bis(3',5'-bis(3'',5''-bis(4-(9H-carbazol-9-yl)butoxy)benzyloxy)benzyloxy)phenyl)methanol [G3-OH] (Scheme 2). Following the general synthesis for method A as described above, the reaction of 0.051 g (1.33mmol) of LAH in 100 mL of THF with a solution of 2.1 g (0.78mmol) of G3-COOR in 20 mL of THF afforded a white solid product in 85% yield. ¹H NMR (CDCl₃): δ (ppm) 8.15 (d, 16H, *J* = 7.5 Hz), 7.53–7.40 (m, 32H), 7.31–7.26 (m, 16H), 6.74 (b, 4H), 6.64 (b, 2H), 6.60 (b, 2H), 6.56 (b, 8H), 6.36 (b, 4H), 4.97 (s, 12H), 4.57 (s, 2H), 4.33 (t, 16H, *J* = 7.0 Hz), 3.86 (t, 16H, *J* = 4.2 Hz), 2.06–2.01 (m, 16H), 1.81–1.77 (m, 16H). ¹³C NMR (CDCl₃): δ (ppm) 160.13, 160.01, 159.90, 143.58, 140.24, 139.25, 139.02, 125.58, 122.73, 120.27, 118.77, 108.58, 106.27, 105.75, 105.50, 101.48, 101.14, 100.75, 69.92, 69.80, 67.39, 64.97, 60.33, 42.49, 26.81, 25.69. Anal. Calcd: C, 80.43; H, 6.25; N, 4.24. Found: C, 80.15; H, 6.28; N, 4.44.

Synthesis of Methyl 3,5-Bis(3',5'-bis(3'',5''-bis(3''',5'''-bis(4-(9H-carbazol-9-yl)butoxy)benzyloxy)benzyloxy)benzyloxy)benzoate [G4-COOR] (Scheme 2). Following the general synthesis for method B as described above, a precooled solution of 0.13 g (0.75 mmol) of methyl 3,5-dihydroxybenzoate, 4 g (1.51 mmol) of G3-OH, and 0.4 g (1.52 mmol) of PPh₃ in THF under sonication was treated with a solution of DIAD (0.31 g, 1.52 mmol) in 1 mL of THF under nitrogen. The solution was sonicated for 4 h to afford a white solid product in 68.6% yield after purification. ¹H NMR (CDCl₃): δ (ppm) 8.10 (d, 32H, *J* = 7.8 Hz), 7.48–7.35 (m, 64H), 7.30 (b, 2H), 7.25–7.20 (m, 32H), 6.79 (b, 1H), 6.71 (b, 8H), 6.69 (b, 4H), 6.61 (b, 6H), 6.51 (b, 16H), 6.32 (b, 8H), 4.92 (b, 28H), 4.27 (t, 32H, *J* = 7.5 Hz), 3.88–3.78 (m, 35H), 2.06–1.94 (m, 32H), 1.78–1.72 (m, 32H). ¹³C NMR (CDCl₃): δ (ppm) 166.59, 160.16, 160.05, 159.65, 140.26, 139.15, 139.00, 138.85, 132.05, 125.60, 122.75, 120.29, 118.77, 108.79, 106.37, 105.79, 101.54, 100.78, 69.83, 67.41, 52.13, 42.50, 26.81, 25.71. Anal. Calcd: C, 80.24; H, 6.18; N, 4.14. Found: C, 80.26; H, 6.10; N, 4.22.

Synthesis of (3,5-Bis(3',5'-bis(3'',5''-bis(3''',5'''-bis(4-(9H-carbazol-9-yl)butoxy)benzyloxy)benzyloxy)benzyloxy)phenyl)methanol [G4-OH] (Scheme 2). Following the general synthesis for method A as described above, the reaction of 38 mg (1 mmol) of LAH in 100 mL of THF with a solution of 3.2 g (0.6 mmol) of G4-COOR in 100 mL of THF afforded a white solid product in 81% yield. ¹H NMR (CDCl₃): δ (ppm) 8.13 (d, 32H, *J* = 7.5 Hz), 7.53–7.48 (m, 32H), 7.44–7.41 (m, 32H), 7.30–7.26 (m, 32H), 6.73–6.71 (m, 12H), 6.63 (b, 9H), 6.55 (b, 16H), 6.36 (b, 8H), 4.96 (b, 28H), 4.56 (b, 2H), 4.35 (t, 32H, *J* = 6.7 Hz), 3.86 (t, 32H, *J* = 5.8 Hz), 2.07–2.00 (m, 32H), 1.82–1.77 (m, 32H). ¹³C NMR (CDCl₃): δ (ppm) 160.19, 160.061, 160.02, 140.30, 139.21, 139.04, 125.62, 122.80, 120.32, 118.81, 108.61, 106.39, 105.84, 101.55, 100.81, 69.96, 67.35, 65.24, 65.03, 42.57, 26.96, 25.74. Anal. Calcd: C, 80.43; H, 6.21; N, 4.16. Found: C, 80.46; H, 6.29; N, 4.19.

Synthesis of Tris(3,5-bis(4-(9H-carbazol-9-yl)butoxy)benzyl)benzene-1,3,5-tricarboxylate [G1-D] (Scheme 3). Following the general synthesis for method B as described above, a precooled solution of 164 mg (0.78 mmol) of benzene-1,3,5-tricarboxylic acid, 1.5 g (2.57 mmol) of G1-OH, and 0.79 g (3 mmol) of PPh₃ in THF under sonication was treated with a solution of DIAD (0.65 g, 3.2 mmol) in 2 mL of THF under nitrogen. The solution was sonicated for 6 h to

afford a white solid product in 71% yield after purification. ^1H NMR (CDCl_3): δ (ppm) 8.86 (s, 3H), 8.07 (d, 12H, $J = 7.5$ Hz), 7.45–7.36 (m, 24H), 7.23–7.18 (m, 12H), 6.48 (d, 6H, $J = 1.5$ Hz), 6.31 (b, 3H), 5.22 (b, 6H), 4.33 (t, 12H, $J = 6.9$ Hz), 3.85 (t, 12H, $J = 6.1$ Hz), 2.05–2.00 (m, 12H), 1.82–1.75 (m, 4H). ^{13}C NMR (CDCl_3): δ (ppm) 164.65, 160.26, 140.37, 137.68, 134.84, 131.23, 125.64, 122.90, 120.38, 119.48, 118.86, 108.63, 106.75, 101.28, 67.58, 67.19, 42.68, 26.92, 25.83. Anal. Calcd: C, 79.47; H, 6.03; N, 4.41. Found: C, 79.12; H, 5.84; N, 4.90.

Synthesis of Tris(3,5-bis(3',5'-bis(4-(9H-carbazol-9-yl)butoxy)benzyloxy)benzyl)benzene-1,3,5-tricarboxylate [G2-D] (Scheme 3). Following the general synthesis for method B as described above, a precooled solution of 38.6 g (0.18 mmol) of benzene-1,3,5-tricarboxylic acid, 0.77 g (0.6 mmol) of G2-OH, and 0.2 g (0.8 mmol) of PPh_3 in THF under sonication was treated with a solution of DIAD (0.18 g, 0.9 mmol) in 2 mL of THF under nitrogen. The solution was sonicated for 6 h to afford a white solid product in 70.6% yield after purification. ^1H NMR (CDCl_3): δ (ppm) 8.81 (s, 3H), 8.05 (d, 24H, $J = 7.2$ Hz), 7.43–7.32 (m, 48H), 7.21–7.16 (m, 24H), 6.64 (d, 6H, $J = 1.2$ Hz), 6.54 (b, 3H), 6.45 (d, 12H, $J = 1.2$ Hz), 6.25 (b, 6H), 5.24 (b, 6H), 4.85 (b, 12H), 4.26 (t, 24H, $J = 7.0$ Hz), 3.77 (t, 24H, $J = 6.0$ Hz), 2.00–1.93 (m, 24H), 1.75–1.68 (m, 24H). ^{13}C NMR (CDCl_3): δ (ppm) 164.57, 160.20, 160.08, 140.31, 140.17, 138.92, 137.74, 134.76, 131.01, 126.03, 125.64, 122.81, 121.96, 120.69, 120.36, 118.83, 108.62, 107.25, 107.14, 105.79, 101.93, 100.77, 100.66, 77.24, 70.01, 67.45, 67.13, 42.60, 26.88, 25.79. Anal. Calcd: C, 79.97; H, 6.10; N, 4.24. Found: C, 80.01; H, 6.00; N, 4.61.

Synthesis of Tris(3,5-bis(3',5'-bis(3'',5''-bis(4-(9H-carbazol-9-yl)butoxy)benzyloxy)benzyloxy)benzyl)benzene-1,3,5-tricarboxylate [G3-D] (Scheme 3). Following the general synthesis for method B as described above, a precooled solution of 40.9 mg (0.19 mmol) of benzene-1,3,5-tricarboxylic acid, 1.7 g (0.64 mmol) of G3-OH, and 0.24 g (0.9 mmol) of PPh_3 in THF under sonication was treated with a solution of DIAD (0.3 g, 1.5 mmol) in 2 mL of THF under nitrogen. The solution was sonicated for 8 h to afford a white solid product in 54% yield after purification. ^1H NMR (CDCl_3): δ (ppm) 8.77 (s, 3H), 8.02 (d, 48H, $J = 7.5$ Hz), 7.40–7.35 (m, 48H), 7.30–7.26 (m, 48H), 7.18–7.14 (m, 48H), 6.61 (b, 18H), 6.51 (b, 9H), 6.42 (b, 24H), 6.22 (b, 12H), 5.15 (b, 6H), 4.80 (b, 36H), 4.19 (t, 48H, $J = 6.6$ Hz), 3.69

(t, 48H, $J = 5.4$ Hz), 2.01–1.80 (m, 48H), 1.73–1.56 (m, 48H). ^{13}C NMR (CDCl_3): δ (ppm) 164.42, 160.13, 160.02, 140.24, 139.05, 138.97, 137.74, 134.61, 130.96, 125.60, 122.75, 120.30, 118.78, 108.58, 106.96, 106.32, 105.78, 101.71, 101.47, 100.69, 77.20, 69.89, 67.37, 67.20, 42.50, 26.92, 25.71. Anal. Calcd: C, 80.21; H, 6.13; N, 4.16. Found: C, 80.00; H, 6.28; N, 4.20.

Synthesis of Tris(3,5-bis(3',5'-bis(3'',5''-bis(3''',5'''-bis(4-(9H-carbazol-9-yl)butoxy)benzyloxy)benzyloxy)benzyloxy)benzyl)benzene-1,3,5-tricarboxylate [G4-D] (Scheme 4). A precooled solution of 16 mg (0.75 μmol) of benzene-1,3,5-tricarboxylic acid, 1.35 g (0.25 mmol) of G4-OH, and 0.13 g (0.5 mmol) of PPh_3 in 15 mL of THF was treated with a dropwise addition of DIAD solution (0.12 g, 0.6 mmol) in 5 mL of THF under nitrogen. The solution was stirred for 1 h after warming the reaction mixture to room temperature. The mixture was then refluxed for 48 h. After cooling the reaction mixture, 0.5 mol % equiv of both PPh_3 and DIAD was added again and refluxed for another 72 h. The final product was obtained as a white solid in 50.9% yield after purification. ^1H NMR (CDCl_3): δ (ppm) 8.68 (s, 3H), 8.02 (d, 96H, $J = 7.2$ Hz), 7.37–7.12 (m, 288H), 6.62 (b, 42H), 6.51 (b, 21H), 6.42 (b, 48H), 6.20 (b, 24H), 5.12 (b, 6H), 4.77 (b, 84H), 4.15 (b, 96H), 3.63 (b, 96H), 1.96–1.76 (m, 96H), 1.68–1.52 (m, 96H). ^{13}C NMR (CDCl_3): δ (ppm) 164.24, 160.09, 159.96, 140.19, 139.10, 139.01, 137.84, 134.23, 130.46, 125.56, 122.68, 120.58, 120.26, 118.75, 108.57, 107.88, 106.82, 106.35, 105.72, 101.42, 100.62, 77.23, 69.83, 67.95, 67.27, 42.20, 26.75, 25.91, 25.62. Anal. Calcd: C, 80.33; H, 6.15; N, 4.12. Found: C, 80.00; H, 6.15; N, 4.21.

Acknowledgment. We are grateful for the partial funding from the Robert A. Welch Foundation (E-1551) and NSF DMR-0504435, NSF-DMR-0602896, and instrument support from DMR-DMR-0315565. Technical support from Maxtek Inc. is also acknowledged.

Supporting Information Available: Experimental details, characterization, and ^1H NMR spectra for all the dendrons and dendrimers reported. This material is available free of charge via the web at <http://pubs.acs.org>.

JA074007T